

Description of Superdeformed Nuclei in the $A \sim 190$ Region by Generalized Deformed $su_q(2)$

H. H. Alharbi*

National Center for Mathematics and Physics, KACST, P.O. Box 6086, Riyadh 11442, Saudi Arabia,

H. A. Alhendi† and F. S. Alhakami

*Department of Physics and Astronomy, College of Science,
King Saud University, P.O. Box 2455, Riyadh 11454, Saudi Arabia.*

The generalised deformed $su_q(2)$ model is applied to 79 superdeformed bands in the region $A \sim 190$. The transition energies and the moments of inertia are calculated within the model. Its validity is investigated by comparing it with the experimental data. Both the standard $su_q(2)$ and the generalized one fail to account for the uprising and the downturn of the dynamic moment of inertia. Both models, however, show remarkable agreement with the available experimental data at low angular frequency ($\hbar\omega \leq 0.25 MeV$).

I. INTRODUCTION

Superdeformed nuclei were first observed in fission isomers in the actinide region [1]. A theoretical explanation of the occurrence of fission isomers, based on shell effect corrections on the liquid drop potential energy surface, was, at then, offered by Strutinsky [2]. The main result was the possible existence of a second minimum in the potential energy as function of nuclear deformation. It is expected nowadays that a third minimum may occur corresponding to hyper-deformed nuclei [3].

A superdeformed rotational band in ^{152}Dy in the form of series of γ -ray energies was first populated in the heavy-ion fusion-evaporation reaction $^{108}\text{Pd}(^{48}\text{Ca}, 4n)^{152}\text{Dy}$ [4]. Since then extensive experimental and theoretical studies have been undertaken. At present superdeformed bands have been observed in various atomic mass region [5]. Most notable regions are at $A \sim 130, 150$, and 190 in which axes ratios are, respectively, close to $1.5 : 1$, $2 : 1$, and $1.7 : 1$ [6]. Superdeformed nuclei enjoy several characteristics that make them of particular interest theoretically and experimentally. For beside their extreme shape and stability against fission they show great regularity in their rotational bands and exhibit some type of universal phenomenon in relation to the existence of nearly identical bands in pairs of nuclei in different mass region and as a result their dynamic moments of inertia are approximately similar [7]. It is expected that the process of the decay of superdeformed nuclei to normal deformed nuclei could proceed through quantum tunneling [8].

For high-spin, superdeformed rotational spectra follow, in general, approximately that of a rigid rotor. Hence the kinematics and the dynamic moments of inertia are nearly constant with slight gradual increase with angular momentum, at low angular frequency. At high angular frequency the dynamic moment of inertia shows irregular behavior.

In this work we consider the q -deformation of the enveloping Lie algebra $su_q(2)$ [9], which has recently attracted much interest for the calculation of rotational spectra of deformed [10] and superdeformed nuclei [11]. The validity of the standard $su_q(2)$ model has, however, been recently questioned [12]. A generalized form of the model which is obtained by replacing the angular momentum spectral expression $I(I+1)$ by $I(I+c)$ has been used to describe successfully the vibrational, transitional and the rotational nuclear spectra of well deformed nuclei [13]. Here we apply this generalized form to the calculation of the rotational transition energies, the kinematic moments of inertia and the dynamic moments of inertia for 79 superdeformed energy bands in the region $A \sim 190$, and compare it with the experimental data. A sensitive measure of the applicability of a model to superdeformed bands is the dynamic moment of inertia. This is because, it is inversely proportional to the difference of the transition energies and these transition energies are closely spaced. The model shows remarkable agreement with the experimental data in the rotational region at low angular frequency ($\hbar\omega \leq 0.25 MeV$). A comparison with the standard $su_q(2)$ model is also made. It is also shown that in addition to the previously predicted deviation of the standard $su_q(2)$ in the case of deformed nuclei, it does so for the case of the superdeformed nuclei considered in this work. It is also concluded,

*Electronic address: alharbi@kacst.edu.sa

†Electronic address: alhendi@ksu.edu.sa / hhalhendi@hotmail.com

contrary to the expectation of reference [13], that in the rotational region the generalized $su_q(2)$ does not in general coincide with the standard one.

In the following section we present a brief description of the model and in the next section we present our results and conclusion.

II. MODEL DESCRIPTION

The $su_q(2)$ algebra is a q deformation of the $SU(2)$ Lie algebra and is generated by the operators, J_- , J_0 , and J_+ , which obey the commutation relations [9][10]:

$$[J_0, J_{\pm}] = \pm J_{\pm}, \quad [J_+, J_-] = [2J_0], \quad (1)$$

with $J_0^\dagger = J_0$, $J_\pm^\dagger = J_\mp$ and $[x]$ is the q number defined as

$$[x] = \frac{q^x - q^{-x}}{q - q^{-1}} \quad (2)$$

In terms of the parameterization $\tau = \ln q$, this equation takes the form:

$$[x] = \frac{e^{\tau x} - e^{-\tau x}}{e^\tau - e^{-\tau}} = \frac{\sinh \tau x}{\sinh \tau} \quad (3)$$

In the $su_q(2)$ formalism it is suggested that rotational spectra of nuclei can be well described by a Hamiltonian proportional to the second-order Casimir operator of the quantum algebra of $su_q(2)$ in a manner similar to that of the $SU(2)$ rotator algebra..

The second-order Casimir operator of $su_q(2)$ is:

$$C_2^q = J_- J_+ + [J_0] [J_0 + 1] \quad (4)$$

with eigenvalues $[I] [I + 1]$.

A deformed q like-rotor is a quantum system described by the $su_q(2)$ invariant Hamiltonian

$$H = \frac{\hbar^2}{2j^{(0)}} C_2^q + E_0, \quad (5)$$

where $j^{(0)}$ is the moment of inertia for $q = 1$ and E_0 the bandhead energy. The parameters $j^{(0)}$ and E_0 are regarded as constants of the model. The rotational energy spectrum can be then expressed as

$$E = \frac{\hbar^2}{2j^{(0)}} \frac{\sin(I|\tau|) \sin[(I+1)|\tau|]}{\sin^2|\tau|} + E_0 \quad (6)$$

where here a pure imaginary $\tau (\equiv \ln q = i|\tau|)$ is assumed.

An extended version of this model is obtained by replacing $I+1$ by $I+c$ where $c > 1$. The addition of the parameter c allows for the description of nuclear anharmonicities in a way similar to that of the Interacting Boson Model and the Generalized Variable Moment of Inertia model. The energy spectrum in this case becomes:

$$E = \frac{\hbar^2}{2j^{(0)}} \frac{\sin(I|\tau|) \sin[(I+c)|\tau|]}{\sin^2|\tau|} + E_0, \quad (7)$$

which contains three parameters: the moment of inertia $j^{(0)}$, the deformed parameter τ , and the anharmonicity parameter c .

In our application of the model in order to fit the three parameters in equation (7) we make use of the transition energies of 79 SD bands in the $A \sim 190$ region that are reported for the nuclei Au, Tl, Bi, Pb, and Po [5]. The kinematic $J^{(1)}$ and the dynamical moment of inertia $J^{(2)}$ are calculated from the following defining relations:

$$J^{(1)} = [(2I - 1)/E_\gamma(I)](\hbar^2 \text{MeV}^{-1}) \quad (8)$$

$$J^{(2)} = 4/[E_\gamma(I + 2) - E_\gamma(I)](\hbar^2 \text{MeV}^{-1}) \quad (9)$$

where the transition energy $E_\gamma(I)$ is

$$E_\gamma(I) = E(I) - E(I - 2), \quad (10)$$

We have used as a quantitative measure for best fit the root mean square (rms) σ defined as:

$$\sigma = \sqrt{\frac{1}{N} \sum_{I=1}^N \left(1 - \frac{E_\gamma^{calc}(I)}{E_\gamma^{exp}(I)}\right)^2}, \quad (11)$$

where N is the number of levels fitted.

III. RESULTS AND CONCLUSION

A representative sample of the fitting parameters and the rms of the two models, for the studied nuclei, are presented in table I and table II. Out of the 79 studied SD bands 20 of them have the anharmonic parameter $c = 1$, which we do not include in the tables, since they lead to no comparison between the two models. These bands are: ^{197}Bi SD, ^{190}Hg SD3, ^{191}Hg SD1, SD4, ^{192}Hg SD2, SD3, ^{193}Hg SD6, ^{195}Hg SD3, ^{193}Pb SD2, ^{195}Pb SD2, ^{197}Pb SD2, SD3, SD4, SD5, SD6, ^{192}Tl SD1, SD2, ^{191}Tl SD2, ^{193}Tl SD3, SD4. In addition 12 SD bands (^{191}Au SD3, ^{189}Hg SD1, ^{190}Hg SD4, ^{192}Hg SD1, ^{194}Hg SD1, ^{195}Hg SD2, ^{190}Tl SD2, ^{193}Tl SD5, ^{193}Pb SD1, ^{195}Pb SD3, ^{196}Pb SD4, ^{198}Pb SD2) have $c > 2$, which are out side the rotational region [13]. Figs. 1-2 clearly illustrate that our calculations of the moments of inertia are in good agreement with experimental data at low angular frequency. Both models give good fit for the kinematic moment of enertia but they show marked disagreement for the dynamic moment of inertia at high angular frequency. The models fail to account for the uprising and the down turn of the dynamic moment of inertia. Comparison of the rms of the studied SD bands, table I and II, for the two models shows a significant improvement in favor of the generalized $su_q(2)$.

Acknowledgement 1 *We would like to thank the referee for his valuable remarks.*

IV. REFERENCES

-
- [1] S. M. Polikanov *et al*, Sov. Phys. JETP **15**, 1016 (1962).
 - [2] V. M. Strutinsky, Nucl. Phys. A **95**, 420 (1967).
 - [3] A. Galindo-Uribarri, *et al*, Phys. Rev. Lett **71**, 231 (1993).
 - [4] P. J. Twin, *et al*, Phys. Rev. Lett **57**, 811 (1986).
 - [5] B. Singh, R. Zywina, and R. B. Firestone, Nucl. Data. Sheets **97**, 241 (2002).
 - [6] D. Ward and P. Fallon, Adv. Nucl. Phys **26**, 167 (2001); R. Janssens and T. Khoo, Ann. Rev. Nucl. Part. Sci. **41**, 321 (1991).

TABLE I: The fitting parameters and rms of the present models (for 1.0 $\leq c \leq 1.5$)

		$su_q(2)$			modified $su_q(2)$			
		$\frac{\hbar^2}{2j(0)}$	τ	$\sigma\%$	$\frac{\hbar^2}{2j(0)}$	τ	c	$\sigma\%$
¹⁹¹ Au	SD1	5.24206	0.00945	0.42239	5.23042	0.00938	1.06323	0.41994
¹⁹¹ Au	SD2	5.38074	0.01073	0.08715	5.32596	0.01041	1.38868	0.07117
¹⁹⁰ Hg	SD1	5.93895	0.01313	0.58702	5.84574	0.01275	1.45	0.41552
¹⁹³ Hg	SD1	5.39158	0.01379	0.17721	5.39158	0.01276	1.02044	0.17721
¹⁹³ Hg	SD2	5.29818	0.01004	0.52098	5.22778	0.00965	1.45	0.35778
¹⁹³ Hg	SD4	5.29818	0.01004	0.52098	5.22778	0.00965	1.45	0.35778
¹⁹³ Hg	SD5	4.83994	0.00219	0.20816	4.81326	0.001	1.17459	0.19576
¹⁹⁴ Hg	SD2	5.28511	0.01007	0.45569	5.20579	0.00958	1.45	0.29270
¹⁹⁵ Hg	SD1	5.26228	0.01035	0.76589	5.19947	0.01004	1.45	0.62843
¹⁸⁹ Tl	SD1	5.52796	0.01065	0.04996	5.49779	0.01042	1.16635	0.03881
¹⁸⁹ Tl	SD2	5.50741	0.01098	0.16131	5.45634	0.01055	1.26928	0.15042
¹⁹¹ Tl	SD1	5.38536	0.01039	0.05602	5.38353	0.01037	1.01021	0.05593
¹⁹² Tl	SD3	5.1029	0.00890	0.25246	5.03279	0.00827	1.40185	0.18759
¹⁹² Tl	SD4	5.1066	0.00903	0.17178	5.06215	0.00861	1.23881	0.12532
¹⁹³ Tl	SD1	5.18845	0.00970	0.27259	5.14984	0.00940	1.21010	0.24470
¹⁹³ Tl	SD2	5.18638	0.00889	0.26542	5.12698	0.00839	1.33399	0.21371
¹⁹⁴ Tl	SD1	5.00301	0.00835	0.12796	4.97268	0.00806	1.18518	0.11626
¹⁹⁴ Tl	SD2	5.00398	0.00849	0.08714	4.97817	0.00821	1.13658	0.05851
¹⁹⁵ Tl	SD1	5.2395	0.00950	0.14559	5.23000	0.00942	1.04212	0.13952
¹⁹⁵ Tl	SD2	5.24353	0.01042	0.21265	5.21783	0.01023	1.12423	0.18672
¹⁹³ Pb	SD3	5.2603	0.00895	0.19961	5.17564	0.00811	1.45755	0.11696
¹⁹³ Pb	SD6	5.34273	0.01056	0.41145	5.25659	0.00985	1.45	0.24225
¹⁹⁴ Pb	SD1	5.62768	0.01231	0.72335	5.50272	0.01128	1.44987	0.40757
¹⁹⁴ Pb	SD2	5.28708	0.01133	0.16664	5.23070	0.01067	1.25752	0.14921
¹⁹⁴ Pb	SD3	5.28808	0.01121	0.13644	5.23187	0.01061	1.27327	0.11896
¹⁹⁵ Pb	SD1	5.05467	0.00596	0.16410	5.00077	0.00496	1.25433	0.06094
¹⁹⁵ Pb	SD4	5.40187	0.01143	0.25481	5.37387	0.01116	1.12594	0.24772
¹⁹⁶ Pb	SD1	5.7067	0.01174	0.23161	5.64178	0.01124	1.26440	0.04316
¹⁹⁶ Pb	SD2	5.42321	0.01111	0.29565	5.34749	0.01039	1.34114	0.23212
¹⁹⁷ Pb	SD1	5.09885	0.00609	0.11375	5.08275	0.00586	1.07249	0.08923
¹⁹⁸ Pb	SD1	5.66046	0.00919	0.33644	5.58475	0.00871	1.45	0.20562

- [7] C. Baktash, B. Haas, and W. Nazarewicz, *Ann. Rev. Nucl. Part. Sci.* **45**, 485 (1995).
[8] C. A. Stafford and B. R. Barrett, *Phys. Rev. C* **60**, 051305(R) (1999); D. M. Cardamone, B. R. Barrett and C. A. Stafford, *arxiv nucl-th /0702072*; T. Lauritsen *et al*; *Phys. Rev. Lett.* **88** 042501 (2002).
[9] L. C. Biedenharn, *J. Phys. A* **22**, L 873 (1989); A. J. Macfarlane, *J. Phys. A* **22**, 4581 (1989).
[10] P. P. Raychev, R. P. Roussev, and Yu. F. Simrnov, *J. Phys. G* **16**, L 137 (1990); S. Iwao, *Progr. Theor. Phys.* **83**, 363 (1990).
[11] D. Bonatsos *et al*, *J. Phys. G* **17**, L67 (1991); R. S. Johal and R. K. Gupta, *J. Phys. G* **25**, L43 (1999).
[12] J. Meng, C. S. Wu, and J. Y. Zeng, *Phys. Rev C* **44**, 2545 (1991).
[13] D. Bonatsos, C. Daskaloyannis, A. Faessler, P. P. Raychev, R. P. Roussev, *Phys. Rev C* **50**, 497 (1994).

TABLE II: The fitting parameters and rms of the present models (for $1.5 \leq c \leq 2.0$)

	$su_q(2)$			modified $su_q(2)$			
	$\frac{\hbar^2}{2J(0)}$	τ	$\sigma\%$	$\frac{\hbar^2}{2J(0)}$	τ	c	$\sigma\%$
^{198}Po SD	5.87348	0.015368	0.37078	5.71292	0.01359	1.52075	0.10810
^{196}Bi SD	5.47304	0.009596	0.61989	5.26217	0.00646	1.82055	0.03724
^{191}Hg SD2	5.28001	0.009649	0.23706	5.18865	0.00899	1.54006	0.08739
^{191}Hg SD3	5.27424	0.010148	0.31120	5.15491	0.00937	1.75194	0.15758
^{193}Hg SD3	5.308	0.010110	0.54763	5.15232	0.00927	1.95203	0.25438
^{194}Hg SD3	5.26475	0.009839	0.55888	5.11966	0.00897	1.88759	0.25922
^{195}Hg SD4	5.08002	0.008086	0.21760	4.98767	0.00753	1.73243	0.13646
^{192}Pb SD	5.73047	0.013809	0.56276	5.5929	0.01268	1.57881	0.47779
^{193}Pb SD4	5.30025	0.010653	0.22269	5.18738	0.00978	1.65015	0.09640
^{193}Pb SD5	5.34677	0.010707	0.36132	5.22763	0.00965	1.58574	0.20445
^{196}Pb SD3	5.4111	0.011044	0.29265	5.29645	0.01002	1.55773	0.15156
^{198}Pb SD3	5.68231	0.011113	0.32830	5.54283	0.00982	1.60574	0.07149
^{194}Tl SD3	5.22953	0.009804	0.30147	5.09825	0.00864	1.72394	0.08790
^{194}Tl SD4	5.23294	0.009887	0.37686	5.08547	0.00847	1.76634	0.12778
^{194}Tl SD5	4.93312	0.008534	0.31105	4.81538	0.00685	1.58204	0.06564
^{194}Tl SD6	4.93169	0.008057	0.24610	4.83214	0.00656	1.50663	0.12430

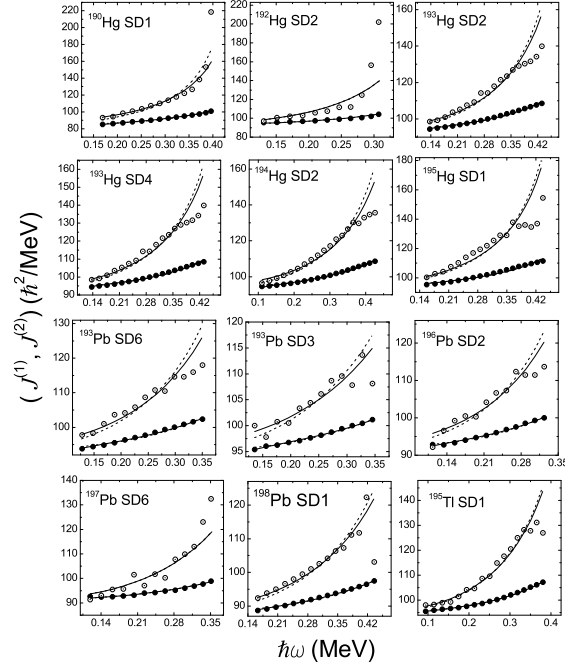


FIG. 1: Comparison between the experimental and theoretical calculation of the Kinematic $J^{(1)}$ (dote) and Dynamic $J^{(2)}$ (circle) moments of inertia versus the rotational frequency ($\hbar\omega$) of a representative sample of superdeformed bands in the $A \sim 190$ region. The modified $su_q(2)$ model (full line) and the nonmodified $su_q(2)$ (dashed line). ^{192}Hg SD2 and ^{197}Pb SD6 have $c = 1$, and c for the rest SDs as in table I.

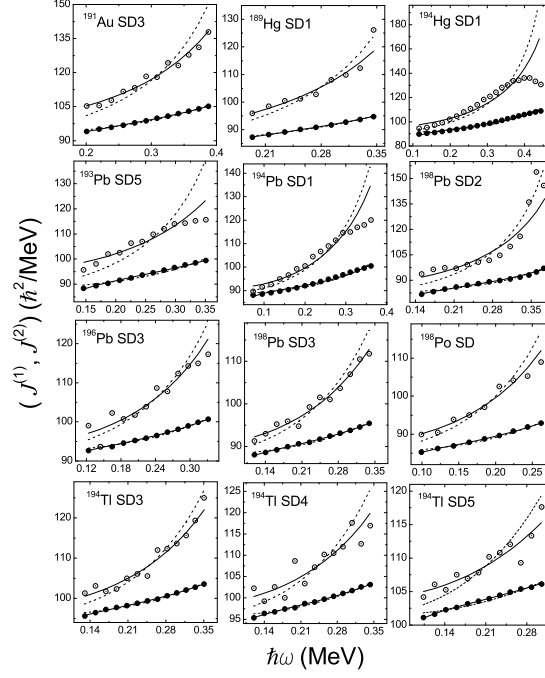


FIG. 2: Comparison between the experimental and theoretical calculation of the Kinematic $J^{(1)}$ (dote) and Dynamic $J^{(2)}$ (circle) moments of inertia versus the rotational frequency ($\hbar\omega$) of a representative sample of superdeformed bands in the $A \sim 190$ region. The modified $su_q(2)$ model (full line) and the nonmodified $su_q(2)$ (dashed line). ^{191}Au SD3, ^{189}Hg SD1, ^{194}Hg SD1, ^{198}Pb SD2 have $c = 3.35953, 2.39011, 2.47371, 2.81838$ respectively; ^{194}Pb SD1 has c as in table I; and c for the rest as in table II.